On Maximum Diversity Order over Doubly-Selective MIMO-OFDM Channes

Qinghai Yang*, Kyung Sup Kwak* *Regular Members*

ABSTRACT

The analysis of maximum diversity order and coding gain for multiple-input multiple-output orthogonal frequency division multiplexing (MIMO-OFDM) systems over time-and frequency-selective (or doubly-selective) channels is addressed in this paper. A novel channel time-space correlation function is developed given the spatially correlated doubly-selective Rayleigh fading channel model.Based on this channel-model assumption, the upper-bound of pairwise error probability (PEP) for MIMO-OFDM systems is derived under the maximum likelihood (ML) detection. For a certain space-frequency code, we quantify the maximum diversity order and deduce the expression of coding gain. In this work, the impact of channel time selectivity is especially studied and a new definition of time diversity is illustrated correspondingly

Key Words : Space-frequency code, MIMO-OFDM, spatial correlation, doubly-selective channel

I. Introduction

Multiple-input multiple-output (MIMO) [1, 2, 3] has recently emerged as one of the most significant technical breakthroughsto provide high rate, reliable and spectrally efficient communications over the wireless medium. Broadband MIMO channels offer spatial diversity due to multiple antennas, as well as frequency diversity due to delay spread. The orthogonal frequency division multiplexing (OFDM) technique significantly reduces the receiver complexity in wireless broadband systems, as the equalizer is just a single-tap filter in the frequency domain. Then MIMO in combination with OFDM, i.e., MIMO-OFDM [4], is proposed as an attractive multi-carrier approach for future broadband wireless systems.

However, most previous considerations on MIMO-OFDM have been restricted to the block time-invariant (i.e., quasi-static) frequency selective channel. This may not be valid at high mobile speeds. This paper extends the channel assumption to be time-varying within a transmission block (one spatial OFDM symbol in this paper). The motivation for doing so is as follows:

- Modeling the time-varying fading within blocksleads to an additional source of diversity, i.e., time diversity [18, 14].
- The conventional block time-invariant fading model severely restricts the block length in the case of fast fading channels. A smaller block length may be a disadvantage for code design, and it usually implies that the channel has to be estimated more frequently. Furthermore, explicitly modeling the channel's time variation within a longer block typically requires fewer parameters than using individual time-invariant channel models for several shorter blocks [19].

With above motivations, maximum diversity (joint

* Graduate School of Information Technology and Telecommunications, Inha University (yangqing_hai@hotmail.com, kskwak@inha.ac.kr)
논문번호 : KICS2005-03-094, 접수일자 : 2005년 3월 3일
※ This work was supported by University IT Research Center Project, Korea(INHA UWB ITRC)

frequency-time diversity) transmission over time- and frequency selective (doubly-selective) channels is addressed in [14] for single input single output channels. On the other hand, time variations within one OFDM symbol block lead to the loss of subcarrier orthogonality, resulting in intercarrier interference (ICI) [12, 20]. Whereas, the work of [15] makesfull use of the time-selective channel as a provider of time diversity while not generating ICI.

For MIMO considerations, the MIMO-OFDM system model under spatially uncorrelated (especially i.i.d.) doubly-selective channels is introduced in [11]. The work of [11] analyzes ICI but with the diversity problem unmentioned. This paper tries to make up with it under a certain space-frequency coded [5, 6, 7, 8, 9] MIMO-OFDM system. Our detailed contributions can be summarized as follows.

- We develop a spatially correlated doubly-selective Rayleigh fading channel model and especially obtain its time-space correlation function.
- Using this channel model, we derive the upper bound of PEP for space-frequency coded MIMO-OFDM system.
- We quantify the maximum diversity order and derive the expression for coding gain. Especially, we focus on the impact of channel time-selectivity on time diversity, and a novel definition of time diversity order is introduced.

The rest of this paper is organized as follows. Sec.II develops the spatially correlated doubly-dispersive Rayleigh fading channel model. Sec.III introduces the data model of space-frequency coded MIMO-OFDM system. Diversity order is quantified in Sec.IV. Sec.V provides simulation results. And Sec.VI concludes this paper.

Notation: we will use $[A]_{m,n}$, $[A]_{.,n}$ and $[A]_{m,.}$ to denote the (m,n)th element, n-th column and m-th row of matrix A, respectively. $Tr(A)$ and $r(A)$ is the trace and rank of matrix A, respectively. I_N is the $N\times N$ identity matrix; $[F]_{m,n} := \frac{1}{\sqrt{N}}e^{-j2\pi mn/N}$ the $N\times N$ FFT matrix. $E\{.\}$ stands for the expectation operator, $\otimes$ for Kronecker product, $\lfloor . \rfloor$ for integer floor and $\lceil . \rceil$ for integer ceiling. The superscripts ^{T,*,H} will denote transpose, conjugate, Hermitian, respectively. min (a,b) denotes the minimum value between a and b. $\mathbb{N}(0,\sigma^2)$ represents the complex Gaussian distribution with mean 0 and varianceσ^2 .

II. Channel Model

In this section, we extend the channel model introduced in [8] to doubly-selective fading conditions. For the case of MIMO channel with M_R receive and M_T transmit antennas, the time- varying impulse response of the channel can be expressed as [6, 10, 8]

$$h_{imp}(t,\tau)=\sum_{l=0}^{L-1}h(t,l)\delta(t-\tau_l) \tag{1}$$

where $\delta(.)$ is the Kronecker delta function; $L=\lfloor w\tau_{DS}\rfloor$ denotes the number of channel taps with w and τ_{DS} representing the signal bandwidth and delay spread, respectively. The $M_R\times M_T$ complex-valued random matrix $h(t,l)$ represents the lth tap at the time t, whose delay is τ_l. Here, one can think of each of the taps as representing a significant scatterer cluster with each of the paths emanating from within the same scatter cluster experiencing the same delay.

According to Eq. (1), the time-varying frequency response of the channel can be easily obtained as

$$H(t,f)=\sum_{l=0}^{L-1}h(t,l)e^{-j2\pi f\tau_l} \tag{2}$$

The discrete-time simulation model can be obtained from the continuous-time structure by sampling the $h_{imp}(t,\tau)$ in t and τ with sampling period T_s (appropriately chosen and equal to the symbol period), e.g., by substituting $\tau_l = lT_s$

and $t=nT_s$. If in the OFDM system the channel is divided into N subchannnels (subcarriers) and the transmitted/received signal is processed by N-point IFFT/FFT, then one block of N symbols is time-limited with approximate bandwidth $1/NT_s$. One can sample $H(t,f)$ with period $1/NT_s$, e.g., $f=k/NT_s$, to obtain

$$H(n,k):=H(nT_s,k/NT_s)=\sum_{l=0}^{L-1} h(nT_s,l)e^{-j2\pi lk/N} \quad (3)$$

where $h(nT_s,l)$ will be notated as $h(n,l):=h(nT_s,l)$ in following discussions.

Without loss of generality, we use $[h(n,l)]_{i,j}$ to represent the l-th tap gain between the j-th transmit antenna and the i-th receive antenna. In order to simplify the analysis in our work, we need to make a few assumptions.

A1) Each $[h(n,l)]_{i,j}$ is modeled as a WSSUS channel, $E[h(n,l)]_{i,j}[h(n,l')]^*_{i,j}=E|[h(n,l)]_{i,j}|^2\delta(l-l')$.
Further using Clarke's two dimensional isotropic scattering model [12], the cross-correlation function between $[h(n,l)]_{i,j}$ and $[h(n',l')]_{i,j}$ can be found as:

$$E[h(n,l)]_{i,j}[h(n',l')]^*_{i,j}= \sigma_l^2\delta(l-l')J_0(2\pi f_D T_s|n-n'|) \quad (4)$$

where σ_l^2 is the total power of the lth tap (derived from the power delay profile of the channel) J_0 is the zero order Bessel function of the first kind; $f_D=v/\lambda$ is maximum Doppler spread: v is the mobile's maximum velocity relative to the base station, λ is the wavelength of RF wave. Notice that the Doppler spread is a measure of time variations in the channel. The larger the value of f_D, the more rapidly the channel changes with time.

A2) The random matrices $h(n,l)(l=0,1,\cdots,L-1)$ have the Gaussian distribution with mean zero and covariance matrix $R_{l,n}\otimes S_{l,n}$, i.e., $E\{\mathrm{vec}(h(n,l))\}=\mathbf{0}_{M_RM_T\times 1}$ and $E\{\mathrm{vec}(h(n,l)).(\mathrm{vec}(h(n,l)))^H\}=R_{l,n}\otimes S_{l,n}$ or $E\{[h(n,l)]_{i,j}[h(n,l)]^*_{i',j'}\}=[R_{l,n}]_{i,i'}[S_{l,n}]_{j,j'}$ $(l=0,\cdots L-1)$, where $R_{l,n}$ and $S_{l,n}$ are $M_R\times M_R$ receive and $M_T\times M_T$ transmit correlation matrices at the l-th tap and time n, respectively. In the following we use the notation $h(n,l)\sim N(0,R_{l,n}\otimes S_{l,n})$ to denote that $h(n,l)$ has matrix-variate Gaussian distribution.

Remark 1: With the **A2**, the MIMO channel is said to be spatially correlated Rayleigh fading. If $R_{l,n}$ and $S_{l,n}$ are identity matrices, i.e., $h(n,l)\sim N(0,I_{M_R}\otimes I_{M_T})$, the channel behaves spatially uncorrelated Rayleigh Fading [13, 16].

If the antennas are arranged in a linear array, $R_{l,n}$ and $S_{l,n}$ are Toeplitz. The l-th tap $h(n,l)$ can be factorized in a 'product' form [8, 13] as

$$h(n,l)=R^{1/2}_{l,n}h_w(n,l)(S^{1/2}_{l,n})^T \quad (5)$$

where $R^{1/2}_{l,n}R^{1/2}_{l,n}=R_{l,n}$ and $S^{1/2}_{l,n}S^{1/2}_{l,n}=S_{l,n}$; $h_w(n,l)$ is an $M_R\times M_T$ matrix with $h_w(n,l)\sim N(0,\sigma_l^2(I_{M_R}\otimes I_{M_T}))$. Note that the σ_l^2 s have been incorporated into the matrices $h_w(n,l)$.

A3) The matrices $R_{l,n}$ and $S_{l,n}$ keep constant within one transmission block (e.g. for one OFDM symbol interval). The time index n is dropped henceforth, i.e., $R_l=R_{l,n}$ and $S_n=S_{l,n}$.

Accordingly, the Eq. (5) can be rewritten as

$$h(n,l)=R^{1/2}_n h_w(n,l)(S^{1/2}_n)^T \quad (6)$$

That is, according to Eq. (6), the time-varying and spatial correlation information of $h(n,l)$ have been sufficiently incorporated into i.i.d. matrices $h_w(n,l)$ and antenna correlation matrices R_l and S_l, respectively. Hence, we say the channel is modeled as an independent time-varying (frequency-dispersive) and spatially correlated channel. Its time-space correlation function is said to be separableand following from Eq. (4), is obtained as,

$$E[h(n,l)]_{i,j}[h(n',l)]^*_{i',j'} = \sigma_l^2 J_0(2\pi f_D T_s|n-n'|)[R_l]_{i,i'}[S_l^T]_{j,j'} \quad (7)$$

and

$$E[h_w(n,l)]_{i,j}[h_w(n',l)]^*_{i',j'} = \sigma_l^2 J_0(2\pi f_D T_s|n-n'|)\delta(i-i')\delta(j-j') \quad (8)$$

Remark 2: It is well known that the channel spatial correlation is relevant to the angle spread and antenna spacing. According to hardware design, the antenna spacing is a constant. On the other hand, since the angle spread changes much more slowly than the channel itself, it is practical to assume that the angle spread keep constant within a transmission block. Hence, it is reasonable in making the assumption 3. The similar assumption is used in several models, for instance, the virtual representation model in [21], discrete-time model in [22] and a generalized model in [23].

Assume that each scatter cluster has a mean angle of departure from the transmit array and a mean angle of arrival at the receive array denoted as $\theta_{T,l}$ and $\theta_{R,l}$, respectively, a cluster angle spread as perceived by the transmitter $\sigma^2_{\theta_{T,l}}$, a cluster angle spread as perceived by the receiver $\sigma^2_{\theta_{R,l}}$. The relative normalized transmit and receive antenna spacing is denoted as $\Delta_T = d_T/\lambda$ and $\Delta_R = d_R/\lambda$, respectively, where d_T and d_R stand for the absolute antenna spacing. Hence, the correlation matrices R_l and S_l are given by(see, e.g., [8] and references therein),

$$[R_l]_{m,n} = \zeta\left((n-m)\Delta_R, \theta_{R,l}, \sigma_{\theta_{R,l}}\right),\ [S_l]_{m,n} = \zeta\left((n-m)\Delta_T, \theta_{T,l}, \sigma_{\theta_{T,l}}\right) \quad (9)$$

where $\zeta(s\Delta,\theta,\sigma_\theta) \approx \exp[-j2\pi s\Delta\cos(\theta)]\cdot\exp[-\frac{1}{2}(2\pi s\Delta\sin(\theta)\sigma_\theta)^2]$ is defined as the fading correlation between two antenna elements spaced $s\Delta$ wavelength apart.

Ⅲ. System Model

Based on the channel assumption in Sec. II, we shall introduce the space-frequency coded MIMO-OFDM system model (Fig. 1) in this section. The

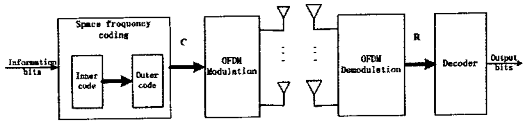

Fig. 1. Block Diagram of System Model

information bits are first encoded by the space-frequency encoder. Define its output $C=[c_0^T,\cdots,c_{N-1}^T]^T$ where $c_k=[c_k^1,\cdots,c_k^{M_T}]^T$ with c_k^i denotes the transmitted symbol from the i-th antenna on the k-th tone [6] and N denotes the number of subcarriers. Here, the space-frequency encoder consists of one inner encoder and one outer encoder (for detail information, refer to [8, 24] and references therein). In this paper, the energy of c_k^i is normalized to unit.

After OFDM demodulation the observed data vector $R=[r_0^T,\cdots,r_{N-1}^T]^T=[r_0^1,\cdots,r_0^{M_R},\cdots,r_{N-1}^1,\cdots,r_{N-1}^{M_R}]^T$ is given by [5, 11]

$$R=\sqrt{E_s}GC+Z \quad (10)$$

where E_s is an energy normalization factor $G=F^{(Rx)}HF^{(Tx)H}$ is an $NM_R \times NM_T$ matrix with $F^{(Rx)}=F\otimes I_{M_R}$, $F^{(Tx)}=F\otimes I_{M_T}$ and H is a block-circulant matrix defined in Eq. (11) with the inner block matrix $h(n,l)$, Z is the equivalent complex-valued AWGN vector with zero mean $E\{Z\}=0_{NM_R\times 1}$ and variance matrix $E\{ZZ^H\}=\sigma_n^2 I_{NM_R}$. Here we denote $Z=[z_0^T,\cdots,z_{N-1}^T]^T$ with $z_k=[c_k^1,\cdots,c_k^{M_R}]^T$. For the OFDM system, we assume that a cyclic prefix of length equal to channel memory is inserted in each transmission block to eliminate inter-symbol interference.

$$\mathbf{H}=\begin{bmatrix} h(0,0) & 0 & \cdots & h(0,2) & h(0,1) \\ h(1,1) & h(1,0) & \cdots & h(1,3) & h(1,2) \\ \vdots & \vdots & \vdots & \vdots & \vdots \\ h(L,L) & (L,L-1) & \vdots & 0 & 0 \\ \vdots & \vdots & \vdots & \vdots & \vdots \\ \vdots & \vdots & \vdots & h(N-2,0) & 0 \\ 0 & 0 & \cdots & h(N-1,1) & h(N-1,0) \end{bmatrix} \quad (11)$$

If we consider an individual received vector r_k, we find

$$r_k=\sqrt{E_s}G_{k,k}c_k+\sqrt{E_s}\sum_{\substack{m=0\\m\neq k}}^{N-1}G_{k,m}c_m+z_k \quad (12)$$

where $G_{k,m}$ is the (k,m)-th block-entity of matrix G and is given by

$$\begin{aligned}\mathbf{G}_{k,m}&=\frac{1}{N}\sum_{n=0}^{N-1}\sum_{l=0}^{L-1}h(n;l)e^{j2\pi n(m-k)/N}e^{-j2\pi ml/N}\\&=\frac{1}{N}\sum_{n=0}^{N-1}H(n,m)e^{j2\pi n(m-k)/N}\end{aligned} \quad (13)$$

That is, the time varying channel destroys the orthognality between subcarriers and gives rise to ICI (i.e., the second term in Eq. (12)) after the FFT process at the receiver. For a detailed discussion on ICI in the MIMO-OFDM system, the interested reader is referred to [11]. However, from the input-output relationship (10), we observe that each transmitted data vector c_k is included in all N received vectors $(r_0, r_1, \cdots, r_{N-1})$, sothe system creates many replicas of each transmitted data vector at the receiver end. Therefore, from another point of view, the time varying channel provides time diversity.

We assume the receiver has perfect channel knowledge while the transmitter has no channel knowledge. The maximum likelihood (ML) decoder computes the vector sequences $\tilde{C}=[\tilde{c}_0^1,\cdots,\tilde{c}_0^{M_T},\cdots,\tilde{c}_{N-1}^1,\cdots,\tilde{c}_{N-1}^{M_T}]^T$ according to

$$\tilde{\mathbf{C}}=\arg\min_{\mathbf{C}}\left\|\mathbf{R}-\sqrt{E_s}\mathbf{GC}\right\|. \quad (14)$$

It is noticed that there is no ICI if an ML decoder is properly chosen. The ICI analysis will be skipped, therefore.

Ⅳ. Diversity Analysis

In this section, we derive the pairwise error probability (PEP) upper bound for space-frequency code taking into account the channel model introduced in sec. II, and then quantify the maximum diversity order.

Assume that C and E are two different space-frequency codewords. Assuming equal transmitted power at all transmitter antennas and ideal channel state information at the receiver, using the Chernoff bound, the PEP of transmitting C and deciding in favor of another codeword E at the ML decoder is upper bounded by [1]

$$P(C\to E|G)\le\exp(-E_s/4\sigma_n^2\|Y\|^2) \quad (15)$$

where $Y=G(C-E)$ is an NM_R-dimensional vector. To continue further analysis, we first make the following observation.

Fact 1: The elements of matrix G have Gaussian distribution.

Proof: According to Assumption 2, the inner block matrices $h(n,l)$ of H in Eq. (13) are complex Gaussian with mean zero and then H is Gaussain with mean zero. With $G=F^{(Rx)}HF^{(Tx)H}$, we conclude that G is Gaussian with mean zero as well.

Now, with ***Fact 1***, Y is a Gaussian random vector with mean zero. We define the covariance matrix of Y as $C_Y=E\{YY^H\}$ and denote $r(C_Y)$ and $\lambda_i(C_Y)$ $(i=1,\cdots,r(C_Y))$ as the rank and eigenvalues of C_Y, respectively. Next, averaging Eq. (15) over the random channel G, we obtain [8]

$$\begin{aligned}P(C\to E)&=E\{P(C\to E|G)\}\\&\le\prod_{i=1}^{r(C_Y)}\frac{1}{1+E_s/4\sigma_n^2\lambda_i(C_Y)}.\end{aligned} \quad (16)$$

We derive (see proof in appendix)

$$C_Y=1/N^2\,\Psi(J\otimes Q)\Psi^H. \quad (17)$$

Define $\Psi=(\Psi_0\otimes I_{M_R},\cdots,\Psi_{N-1}\otimes I_{M_R})$ with size $NM_R\times N^2M_R$ where Ψ_n are $N\times N$ inner block matrices with elements $[\Psi_n]_{i,j}=e^{-j\pi n(i-j)/N}$, $i,j,n=0,\cdots N-1$; J is an $N\times N$ matrix with elements $[J]_{i,j}=J_0(2\pi f_DT_s|i-j|)$. The $NM_R\times NM_R$ matrix $Q=\sum_{l=0}^{L-1}\sigma_l^2[D_lX^TS_lX^*D_l^*]\otimes R_l$ with l-th tap power σ_l^2, $D_l = diag(1, \cdots, e^{-j2\pi l(N-1)/N})$ and the $M_T \times N$ pairwise error codeword matrix $X = [X_0, X_1, \cdots X_{N-1}]$ with column vectors $X_n = [c_n^1 - e_n^1, \cdots, c_n^{M_T} - e_n^{M_T}]^T$, i.e., $\text{vec}(\mathbf{X}) = \mathbf{C} - \mathbf{E}$. The Eq. (17) is the key result of this paper.

In this section we focus on the high SNR regime, i.e., $E_s/4\sigma_n^2 \gg 1$. Then, it follows from inequality Eq. (16) that

$$\mathbf{P}(\mathbf{C} \to \mathbf{E}) \le \left(\frac{E_s}{4\sigma_n^2}\right)^{-r(C_Y)} \prod_{i=0}^{r(C_Y)-1} \lambda_i^{-1}(C_Y) \quad (18)$$

According to the definition in [1] and Eq. (18), the diversity order achieved by the space-frequency code is provided by the minimum rank of C_Y, i.e., $r(C_Y)$ over all codeword pairs $\{C, E\}$, while the coding gain is defined as the minimum of $[\prod_{i=1}^{r(C_Y)} \lambda_i(C_Y)]^{\frac{1}{r(C_Y)}}$.

Diversity order: Following the fact $\Psi\Psi^H = N^2 I_{NM_R}$ in Eq. (17), we obtain $r(\Psi) = NM_R$. Let us next set $\Psi = N.U\Lambda V$ where $\Lambda = [I_{NM_R} \vdots 0]$, U and V are $NM_R \times NM_R$ and $N^2M_R \times N^2M_R$ unitary matrices, respectively. We further set $J \otimes Q = A \triangle B^H$, where $\triangle$ is an $N^2M_R \times N^2M_R$ diagonal matrix containing the eigenvalues of $J \otimes Q$, A and B^H are $N^2M_R \times N^2M_R$ unitary matrices. With these definitions, we then rewrite C_Y as

$$C_Y = U\Lambda(V\mathrm{A})\Delta(B^H V^H)\Lambda^T U^H \quad (19)$$

Now, we can obtain the rank of C_Y as $r(C_Y) = \min(r(\Lambda), r(\triangle)) = \min(r(\Psi), r(J \otimes Q))$. Using the property of Kronecker product $r(J \otimes Q) = r(J).r(Q)$, we finally determine $r(C_Y) = \min(NM_R, r(J).r(Q))$.

According to [8] we have known that $r(Q)$ is affected by the transmitted codewords, the correlations of transmit and receive antennas and the number of frequency-selective channel paths, and its upper bound is found as $r(Q) \le LM_RM_T$.

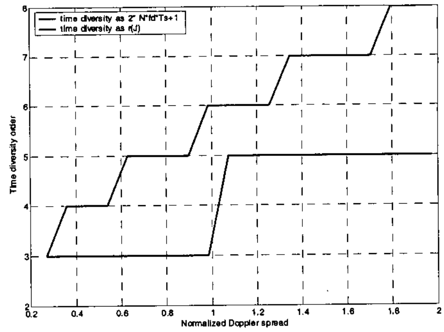

Fig. 2. Effects of Doppler Spread on the Rank of J and Time Diversity Order

In the following, in order to keep the presentation simple, we assumethe number of OFDM subcarrier $N \ge r(J)LM_T$. Hence, $r(J).r(Q) \le NM_R$ and we can obtain the total diversity order as

$$r(C_Y) = r(J) \cdot r(Q). \quad (20)$$

Eq. (20) declares the linear relationship between the total diversity order achieved by the space frequencycode over the doubly-selective channel, i.e., $r(C_Y)$ and the total diversity order achieved over the time-selective channel [8], i.e., $r(Q)$. As the term $r(J)$ is sufficiently determined by Doppler spread and the number of OFDM subcarriers, we define it the maximum time diversity order in this paper. It is shown in Fig. 2 that as the normalized Doppler spread increased, the channel becomes time-selective and the time diversity, i.e., $r(J)$ tends to be increased correspondingly.

Whereas, for SISO channel, [14] has defined the time diversity order as $2\lceil Tf_D \rceil + 1$(see also Fig. 2.) with the signal duration T($T = NT_s$) and Doppler spread f_D. And it is declared that the relatively small Doppler-spread encountered in practice could be even leveraged into significant diversity gains. Compared with the SISO case, the time diversity order with $r(J)$ turns to be saturated as the Doppler spread is increased continually, namely, $r(J) \le N$.

Remark 3: From Eq. (20) we observe that the achievable time diversity order, i.e., $r(J)$ is independent with $r(Q)$. Thus the conclusions on

$r(Q)$ in work [8] can be directly applied to our work. The key points of these conclusions include that space-frequency coding approach can exploit both frequency diversity and spatial diversity in MIMO-OFDM systems. Nevertheless, we don't say the matrix J is independent with the system, since it is derived based on the space-frequency coded MIMO-OFDM under our channel assumptions.

Coding gain: Following from Eq. (19) and Eq. (20), we observe that the eigenvalues of $r(C_Y)$, $\lambda_i(C_Y)=\lambda_i(J\otimes Q)$, i.e., the nonzero elements of iagonal matrix $\triangle$ in Eq. (19). We write $\lambda_i(C_Y) = \lambda_u(J)\lambda_w(Q)$, $i=1,\cdots,r(C_Y)$, $u=1,\cdots,r(J)$ and $w=1,\cdots,r(Q)$, where $\lambda_u(J)$ and $\lambda_w(Q)$ are the eigenvalues of matrix J and Q, respectively. We decompose the coding gain

$$\left(\prod_{i=0}^{r(C_Y)-1}\lambda_i(C_Y)\right)^{1/r(C_Y)}=\left(\prod_{u=0}^{r(\mathbf{J})-1}\lambda_u(\mathbf{J})\right)^{1/r(\mathbf{J})}\cdot\left(\prod_{w=0}^{r(\mathbf{Q})-1}\lambda_w(\mathbf{Q})\right)^{1/r(\mathbf{Q})} \tag{21}$$

Now, in the above equation, we observe that the latter decomposed term happens to be the coding gain discussed in [8], whereas, the former one is the contribution for the coding gain introduced by the time-varying channel, and it is definitely determined by the Doppler spread. Following from the arithmetic-geometric mean inequality [17], we obtain the upper bound as

$$\left(\prod_{u=0}^{r(\mathbf{J})-1}\lambda_u(\mathbf{J})\right)^{1/r(\mathbf{J})}\le\frac{1}{r(\mathbf{J})}\underbrace{\sum_{u=0}^{r(\mathbf{J})-1}\lambda_u(\mathbf{J})}_{\mathrm{Tr}(\mathbf{J})=N}=\frac{N}{r(\mathbf{J})} \quad . \tag{22}$$

So far, it is difficult to further quantify the coding gain.

In this section, we conclude that the maximum diversity order achieved by space-frequency code under the spatially correlated doubly-dispersive Rayleigh fading channel is $r(C_Y)=r(J).r(Q)$, where $r(J)$ is fully determined by the Doppler spread and N, and $r(Q)\le LM_RM_T$ incorporates the frequency and spatial diversity, respectively. As this paper considers the high SNR case, it is noted that the total diversity order has the dominating contribution to improve the performance. Next, recall that our results are derived with the ML(optimum) decoding assumption. In fact, the ML decoding is not realistic for a space-frequency coded MIMO-OFDM system due to its extreme computation complexity. Generally, sub-optimum decoding, for instance, MMSE equalizer can be employed to reduce the complexity, though leading to some time diversity loss. Therefore, our result is the upper bound of the full diversity order offered by our space-frequency coded MIMO-OFDM transmissio

V. Simulation Results

In this section, we present simulations to test the diversity provided by the doubly-selective MIMO channels. Compared with the results in [8], the impact of time diversity on the system-performance is especially discussed in this example. We simulated system with the channel model described in sec. II, in which we select $M_R=M_T=2$, $N=128$, $f_c=900MHz$. With the maximum mobile velocity $v=168km/h$, the maximum Doppler spread is $f_D=140Hz$, $L=4$ with $\sigma_0^2=\sigma_1^2=\sigma_2^2=\sigma_3^2=1/4$. As the average energy of the transmit symbols is assumed to be 1, the signal to noise ratio at each received antenna is defined as $SNR=10\log10(M_TE_s/\sigma_n^2)\leftarrow$. And each point of the curve of OFDM symbol error rate is averaged over 2,000 channel realizations.

For the space-frequency encoder, we employ the 16-states 4-PSK space-time trellis code proposed in [1] as inner code, and the outer code A_t in [24] with dimension $N\times N/2$. We assume channel state information is required at the receiver. Due to the high complexity, we avoid to use the ML decoding. An MMSE equalizer is adopted after the OFDM demodulation, and then the viterbi decoder is applied to decode the space-time trellis code. Here, we point out that the MMSE is not able to collect the full diversity order.

To see the spatial correlation effect, we use three spatially correlated channel cases: no antenna correlation (i.i.d.) channel, receiver-correlation-only (S_l is identity) channel by generating R_l with $\Delta_R=0.2$, $\theta_{R,l}=\pi/4$ and $\sigma_{\theta_{R,l}}=0.250$; transmit-correlation-only channel (R_l is identity) by generating S_l with $\Delta_T=0.5$, $\theta_{T,l}=\pi/4$ and $\sigma_{\theta_{T,l}}=0.25$, respectively.

In order to test the time-diversity quantified by $\gamma(J)$, we compare the performance of two cases: $\gamma(J)=4$ and $\gamma(J)=7$. According to the curve of $\gamma(J)$ vs. normalized Doppler spread (NDS) in Fig.2, we select T_s properly with $T_s=NDS/(Nf_D)$. In this simulation, 3×10^{-5} and 9×10^{-5} are chosen for T_s corresponding to $\gamma(J)=4$ and $\gamma(J)=7$, respectively.

We draw the curves of OFDM symbol error rate vs. SNR in Fig. 3. It is shown that, the spatial correlation decreases the system performance and i.i.d. channel offers the best performance among the three spatial cases. The case of transmit-correlation-only has better performance over the case of receive-correlation-only. The asymmetry is introduced via different transmit and receive antenna spacing for the cases of transmit-correlation-only and receive-correlation-only, respectively.

As expected, for a certain spatial correlation case, better performance is achieved with the time diversity $\gamma(J)=7$ than that with $\gamma(J)=4$. Observing the slope of the curves in Fig. 3, we find that

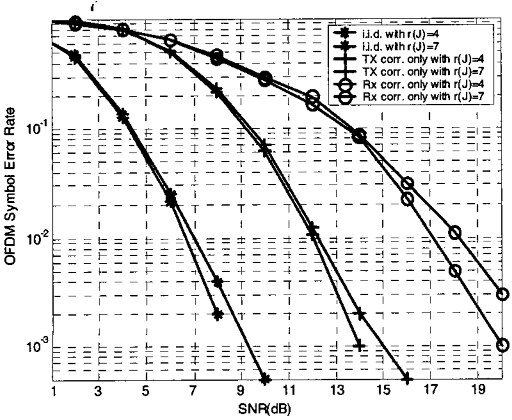

Fig. 3. OFDM symbol error rate vs. SNR

the diversity contributes especially in high SNR cases. Sharper slope happens to the case of $\gamma(J)=7$, while SNR begins from 6dB for i.i.d channel, 12dB for transmit-correlation-only channel and 14dB for receive-correlation-only channel, respectively. Note that due to the MMSE equalizer, some interference is introduced and some time diversities are lost as well. Thus, the time diversity orders shown in Fig.3 may not be the exact values as 7 or 4. However, from their curve slopes, we also can make some insights for quantifications. For instance, as the OFDM symbol error rate is 0.5×10^{-3}, there is at least 2dB performance difference between the cases with $\gamma(J)=7$ and $\gamma(J)=4$.

Ⅵ. Conclusions

The maximum diversity order is developed for the space-frequency coded MIMO-OFDM over spatially correlated doubly-dispersive Rayleigh channel. By deriving the PEP upper bound, we quantify the maximum diversity order and give the expression of coding gain. The impact of channel time-selectivityon the system performance is particularly studied. A novel definition of time-diversity in MIMO-OFDM systems is pro- posed. Such time-diversity is independent with the frequency diversity and space diversity achieved by the space-frequency coded MIMO-OFDM in frequency-selective channe.

APPENDIX

According to the block-matrix $[G]_{k,m}$ given in Eq. (13), we rewrite G

$$\begin{aligned}\mathbf{G} &= \frac{1}{N}\sum_{n=0}^{N-1}\sum_{l=0}^{L-1}(\Psi_n D_l)\otimes h(n,l)\\ &= \frac{1}{N}\sum_{n=0}^{N-1}\sum_{l=0}^{L-1}(\Psi_n\otimes I_{M_R})(D_l\otimes h(n,l))\\ &= \frac{1}{N}\sum_{n=0}^{N-1}(\Psi_n\otimes I_{M_R})\sum_{l=0}^{L-1}D_l\otimes h(n,l) \qquad (25)\end{aligned}$$

where Ψ_n is an $N\times N$ matrix with the elements $[\Psi_n]_{i,j}=e^{-j\pi n(i-j)/N}$, for $i,j,n=0,\cdots,N-1$

and $D_l = diag(1, \cdots, e^{-j2\pi l(N-1)/N})$. In Eq. (25) we write

$$\sum_{l=0}^{L-1} D_l \otimes h(n,l) = \text{diag}\{\sum_{l=0}^{L-1} h(n,l), \sum_{l=0}^{L-1} h(n,l)e^{-j2\pi l/N}, \cdots, \sum_{l=0}^{L-1} h(n,l)e^{-j2\pi l(N-1)/N}\}$$
$$= \text{diag}\{H(n,0), H(n,1), \cdots, H(n,N-1)\} \quad (26)$$

Define $X = [X_0, X_1, \cdots X_{N-1}]$ with column vectors $X_n = [c_n^1 - e_n^1, \cdots, c_n^{M_T} - e_n^{M_T}]^T$, i.e., $\text{vec}(\mathbf{X}) = \mathbf{C} - \mathbf{E}$. And rewrite the vector Y in Eq.(15) as

$$\mathbf{Y} = \mathbf{G}(\mathbf{C} - \mathbf{E})$$
$$= \frac{1}{N}\sum_{n=0}^{N-1}(\Psi_n \otimes I_{M_R}) \cdot \text{diag}\{H(n,0), H(n,1), \cdots, H(n,N-1)\}[X_0^T, X_1^T, \cdots, X_{N-1}^T]^T$$
$$= \frac{1}{N}\sum_{n=0}^{N-1}(\Psi_n \otimes I_{M_R})\begin{bmatrix} H(n,0)X_0 \\ H(n,1)X_1 \\ \vdots \\ H(n,N-1)X_{N-1} \end{bmatrix} \quad (27)$$

For easy expression, we make the notation

$$\mathbf{H}_n = \begin{bmatrix} H(n,0)X_0 \\ H(n,1)X_1 \\ \vdots \\ H(n,N-1)X_{N-1} \end{bmatrix}.$$

Hence Eq. (27) can be written as $Y = 1/N \sum_{n=0}^{N-1}(\Psi_n \otimes I_{M_R})H_n$. We can easily find that

$$\mathbf{YY}^H = \frac{1}{N}\sum_{n=0}^{N-1}(\Psi_n \otimes I_{M_R})\mathbf{H}_n \frac{1}{N}\sum_{n'=0}^{N-1}\mathbf{H}_{n'}^H(\Psi_{n'} \otimes I_{M_R})^H$$
$$= \frac{1}{N^2}\sum_{n=0}^{N-1}\sum_{n'=0}^{N-1}(\Psi_n \otimes I_{M_R})\mathbf{H}_n\mathbf{H}_{n'}^H(\Psi_{n'} \otimes I_{M_R}) \quad (28)$$

Next, the covariance matrix of Y is (note $E\{\mathbf{Y}\} = 0_{NM_R \times 1}$),

$$C_Y = E\{\mathbf{YY}^H\} = \frac{1}{N^2}\sum_{n=0}^{N-1}\sum_{n'=0}^{N-1}(\Psi_n \otimes I_{M_R})E\{\mathbf{H}_n\mathbf{H}_{n'}^H\}(\Psi_{n'} \otimes I_{M_R}) \quad (29)$$

Here,

$$E\{\mathbf{H}_n\mathbf{H}_{n'}^H\} = E\left\{\begin{bmatrix} H(n,0)X_0 \\ H(n,1)X_1 \\ \vdots \\ H(n,N-1)X_{N-1} \end{bmatrix} \cdot \left[X_0^H H^H(n',0), X_1^H H^H(n',1), \cdots, X_{N-1}^H H^H(n',N-1)\right]\right\}. \quad (30)$$

In the above Equation, the (i,j)th block matrix is given by $E\{H(n,i)X_iX_j^H H^H(n',j)\}$.

$$E\{H(n,i)X_iX_j^H H^H(n',j)\} = E\left\{\sum_{l=0}^{L-1} h(n,l)e^{-j2\pi li/N}X_iX_j^H \sum_{l'=0}^{L-1} h^H(n',l')e^{j2\pi l'j/N}\right\}$$
$$= E\left\{\sum_{l=0}^{L-1} e^{-j2\pi li/N}R_l^{1/2}\underbrace{h_w(n,l)\left(S_l^{1/2}\right)^T X_iX_j^H \left(S_l^{1/2}\right)^T}_{\Gamma} h_w^H(n',l)R_l^{1/2}e^{j2\pi lj/N}\right\}$$
$$= \sum_{l=0}^{L-1} e^{-j2\pi li/N}R_l^{1/2} \cdot E\{h_w(n,l)\Gamma h_w^H(n',l)\} \cdot R_l^{1/2}e^{j2\pi lj/N} \quad (31)$$

Following from Eq. (8), we obtain,

$$E\{h_w(n,l)\Gamma h_w^H(n',l)\} = \sigma_l^2 J_0(2\pi f_D T_s |n-n'|) \cdot \left(\sum_{s=1}^{M_R}[\Gamma]_{s,s}\right) \cdot I_{M_R}. \quad (32)$$

Denote $\alpha_{p,q} = [(S_l^{1/2})^T]_{p,q}$, $p, q = 1, \cdots, M_T$.

$$\sum_{s=1}^{M_T}[\Gamma]_{s,s} = \sum_{s=1}^{M_T}\sum_{p=1}^{M_T}\sum_{q=1}^{M_T}\alpha_{s,p}x_i^p(x_j^q)^*\alpha_{q,s} = \sum_{p=1}^{M_T}\sum_{q=1}^{M_T}x_i^p(x_j^q)^*\sum_{s=1}^{M_T}\alpha_{q,s}\alpha_{s,p}$$
$$= \sum_{p=1}^{M_T}\sum_{q=1}^{M_T}x_i^p(x_j^q)^*[S_l^T]_{q,p} = \sum_{p=1}^{M_T}\sum_{q=1}^{M_T}x_i^p(x_j^q)^*[S_l]_{p,q} = X_i^T S_l X_j^* \quad (33)$$

With the aid of Eq. (32) and Eq. (33), we further simplify Eq. (31) as

$$E\{H(n,i)X_iX_j^H H^H(n',j)\} = \sum_{l=0}^{L-1}\sigma_l^2 J_0(2\pi f_D T_s |n-n'|)e^{-j2\pi li/N}R_l^{1/2} \cdot X_i^T S_l X_j^* \cdot R_l^{1/2}e^{j2\pi lj/N}$$
$$= J_0(2\pi f_D T_s |n-n'|)\sum_{l=0}^{L-1}\sigma_l^2 e^{-j2\pi li/N}\underbrace{X_i^T S_l X_j^*}_{\text{scalar}} \cdot R_l e^{j2\pi lj/N} \quad (34)$$

Thus, according to Eq. (34), we simplify the Eq. (30) which is written as

$$E\{\mathbf{H}_n\mathbf{H}_{n'}^H\} = J_0(2\pi f_D T_s |n-n'|)\sum_{l=0}^{L-1}\sigma_l^2(D_l X^T S_l X^* D_l^*) \otimes R_l. \quad (35)$$

The covariance matrix of Y can be obtained finally and rewritten in a compact matrix form

$$C_Y = E\{\mathbf{YY}^H\} = \frac{1}{N^2}\Psi(\mathbf{J} \otimes \mathbf{Q})\Psi^H \quad (36)$$

where $\Psi = (\Psi_0 \otimes I_{M_R}, \cdots, \Psi_{N-1} \otimes I_{M_R})$ with size $NM_R \times N^2M_R$; $Q = \sum_{l=0}^{L-1}\sigma_l^2[D_l X^T S_l X^* D_l^*] \otimes R_l$ with l-th tap power σ_l^2; J is an $N \times N$ matrix with elements $[J]_{i,j}=J_0(2\pi f_D T_s|i-j|)$ for $i,j=0,\cdots,N-1$.

REFERENCE

〔1〕 V. Tarokh, N. Seshadri, and A. R. Calderbank, "Space-time codes for high data rate wireless communication: Performance criterion and code construction," IEEE Trans. Inf. Theory, vol. 44, pp. 744-765, March 1998.

〔2〕 S. M. Alamouti, "A simple transmit diversity techniques for wireless communications," IEEE J. Select. Areas Com., vol. 16, pp. 1451 - 1458, Oct. 1998.

〔3〕 G. J. Foschini, "Layered space-time architecture for wireless communication in a fading environment when using multi-element antennas," Bell Labs Tech. J., pp. 41-59, Autumn 1996.

〔4〕 G.G.Raleigh and J. M. Cioffi, "Spatio-temporal coding for wireless communication," IEEE Trans. Comm., vol. 46, no. 3, pp.357-366, 1998.

〔5〕 H. Blcskei, D. Gesbert and A. J. Paulraj, "On the capacity of OFDM-based spatial multiplexing systems," IEEE Trans. Comm., vol. 50, pp. 225-234, Feb. 2002.

〔6〕 B. Lu and X.Wang, "Space-time code design in OFDM systems," in Proc. IEEE GLOBECOM2000, pp. 1000-1004, Nov. 2000.

〔7〕 Z. Liu, Y. Xin and G. B. Giannakis, "Space-Time-Frequency Coded OFDM over Frequency-Selective Fading Channels", IEEE Trans. on Signal Processing, Vol. 50, No.10, pp.2465-2476, Oct. 2002.

〔8〕 H. Blcskei, M. Borgmann, and A. J. Paulraj, "Impact of the Propagation Environment on the Performance of Space-Frequency Coded MIMO-OFDM", IEEE J. Select. Areas Comm., Vol. 21, NO.3, pp. 427-439, Apr. 2003.

〔9〕 S. Zhou and G. B. Giannakis, "Space-time coding with maximum diversity gains over frequency-selective fading channels," IEEE Signal Processing Letters, vol. 8, pp. 269-272, Oct. 2001.

〔10〕 K. Liu, T. Kadous and A. M. Sayeed, "Optimal Time-Frequency Signaling for Rapidly Time-Varying", Proc. ICASSP 2001, May 2001.

〔11〕 A. Stamoulis, S. N. Diggavi and N. Al-Dhahir, "Intercarrier Interference in MIMO OFDM", IEEE trans. on Signal Processing, Vol. 50, No. 10, pp. 2451-2464, Oct. 2002.

〔12〕 J. Li and M. Kavehrad, "Effects of Time Selective Multipath Fading on OFDM Systems for Broadband Mobile Applications", IEEE Comm. Letters, Vol. 3, No. 12, pp.332-334, Dec,1999.

〔13〕 D.S. Shiu, G. J. Foschini, M. J. Gans and J. M. Kahn, "Fading Correlation and Its Effect on the Capacity of Multielement Antenna Systems", IEEE Trans. on Comm., Vol. 48, No. 3, pp. 502-513, Mar. 2000.

〔14〕 X. Ma and G. B. Giannakis, "Maximum Diversity Transmissions over Doubly-Selective Wireless Channels", IEEE Trans. on Informa. Theory, vol. 49, no. 7, pp. 1832-1840, July 2003.

〔15〕 Y. S. Choi, P. J. Voltz and F. A. Cassara, "On Channel Estimation and Detection for Multicarrier Signals in Fast and Selective Rayleigh Fading Channels," IEEE Trans. on Commun., Vol. 49, pp. 1375-1387, Aug. 2001.

〔16〕 C. Chuah, D. Tse, J.M.Kahn and R.A. Valenzuela, "Capacity Scaling in MIMO Wireless Systems Under Correlated Fading", IEEE Trans. on Informa. Theory, vol. 48, no. 3, pp. 637-650, Mar. 2002.

〔17〕 S.Boyd, "Convex Optimization", Cambridge University Press, Dec. 2002.

〔18〕 A. M. Sayeed and B. Aazhang, "Joint Multipath-Doppler Diversity in mobile wireless communications", IEEE Trans. on Commun., Vol. 47, pp. 123-132, Jan. 1999.

〔19〕 H. Artes and F. Hlawatsch, "Space-time Matrix Modulation: Extension to Unknown Doubly Selective MIMO Channels," IEEE ICASSP 2003.

〔20〕 E. Chiavaccini and G. M. Vitetta, "Error

Performance of OFDM Signaling Over Doubly-Selective Rayleigh Fading Channels," IEEE Commun. Letters, Vol. 4, pp. 328-330, Nov. 2000.

[21] A. M. Sayeed and V.V.Veeravalli, "The Essential Degree of Freedom in Space-Time Fading Channels," PIMRC'02, pp.1512-1516, Sep. 2002.

[22] C. Xiao, J. Wu, S.Y. Leong, Y.R. Zheng and K.B. Letaief, "A Discrete-Time Model for Spatio-Temporally Correlated MIMO WSSUS Multipath Channels," IEEE WCNC 2003, Vol. 1, pp. 354-358, Mar. 2003.

[23] W. Weichselberger, M. Herdin, H. Ozcelik and E. Bonek, "A Stochastic MIMO Channel Model with Joint Correlation of Both Link Ends," Submitted to IEEE Trans. on Wireless Comm., Aug. 2003.

Qinghai Yang ***Regular Member***

He received B.S. Communication Engineering from Shandong Univ. of Technology in 1998 and M.S. in Information & Communication Systems from Xidian Univ., China in 2001. Currently working towards his Ph. D at Inha University, Korea. His research interest lies in the fields of Signal Processing for wireless communications, including multiuser MIMO/OFDM, UWB and their cross layer design.

Kyung Sup Kwak ***Regular Member***

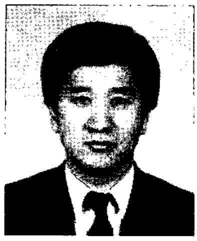

He received his B.S. and M.S. in Electrical Engineering from Inha University, in 1977 and 1979, respectively. And M.S. in Electronics from University of South California in 1981 and Ph. D. in Comm. Engineering from University of California, San Diego, in 1988. He was a researcher at US Hughes Network Systems from Feb. 1988 to Feb. 1989 and a researcher at IBM Network Analysis Center from Feb. 1989 to Mar. 1990. Since then, he was a professor at Inha University, Korea. He was the Director for IEEE Seoul Section from Jan. 1995 to Nov. 1999 and the Dean of the Graduate School of IT&Telecom, Inha University. He has been the Vice-president of Korean Institute of Communication Science since Jan. 2002. His research Interests include Satellite Communication, Multimedia Communication, UWB, wireless communications.